Published in final edited form as:
Langmuir. 2012 October 2; 28(39): 13877–13882. doi:10.1021/la3025149.

On-Surface Assembly of Coiled-Coil Heterodimers

Simon J. White[†], **D. William A. Morton**[‡], **Boon Chong Cheah**[‡], **Agnieszka Bronowska**[§], **A. Giles Davies**[‡], **Peter G. Stockley**[†], **Christoph Wälti**[*,‡], and **Steven Johnson**[*,‖]

[†]Astbury Centre for Structural Molecular Biology, University of Leeds, Leeds LS2 9JT, United Kingdom

[‡]School of Electronic and Electrical Engineering, University of Leeds, Leeds LS2 9JT, United Kingdom

[§]Heidelberg Institute for Theoretical Studies gGmbH, D-69118 Heidelberg, Germany

[‖]Department of Electronics, University of York, Heslington, York YO10 5DD, United Kingdom

Abstract

The coiled coil is a widespread protein motif responsible for directing the assembly of a wide range of protein complexes. To date, research has focused largely on the solution phase assembly of coiled-coil complexes. Here, we describe an investigation into coiled-coil heterodimer assembly where one of the peptides is immobilized directly onto a gold electrode. Immobilization is achieved by the introduction of a unique cysteine residue at the C terminus, allowing for covalent and orientated attachment to a thiol-reactive surface, here the gold electrode. We show an electrochemical impedance of the resulting self-assembled polypeptide monolayer around $|Z| = 4 \times 10^4\ \Omega\ cm^2$ at 100 mHz with a minimum phase angle of −84°, consistent with the formation of a densely packed, insulating layer. The thickness of the peptide monolayer, as measured using ellipsometry, is around 3 nm, close to that expected for a self-assembled monolayer assembled from helical peptides. Crucially, we find that the efficiency of dimerization between a peptide in solution and its coiled-coil partner peptide immobilized on a surface is strongly dependent upon the density of the immobilized peptide layer, with dimer assembly being strongly suppressed by high-density peptide monolayers. We thus develop an approach for controlling the density of the immobilized peptide by diluting the monolayer with a thiolated, random-coil peptide to modulate dimerization efficiency and demonstrate electrochemical detection of highly specific, coiled-coil heterodimer on-surface assembly.

Graphical abstract

[*]**Corresponding Author** c.walti@leeds.ac.uk (C.W.); steven.johnson@york.ac.uk (S.J.).

The authors declare no competing financial interest.

Europe PMC Funders Author Manuscripts

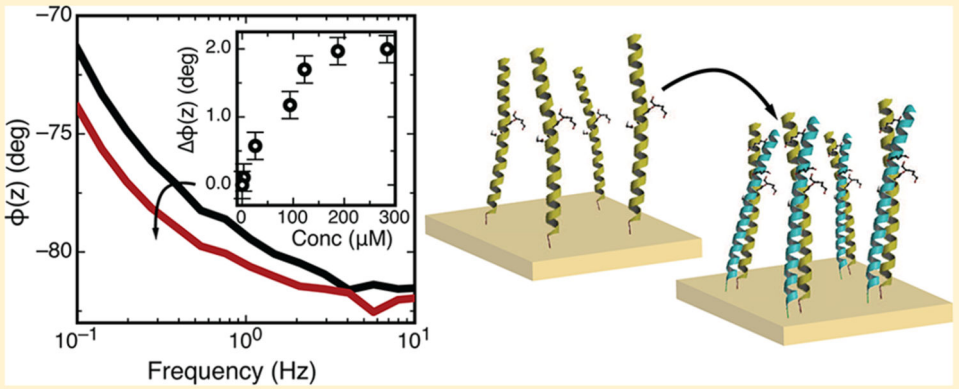

INTRODUCTION

The binding of biological, molecular, and nanoscale components from solution onto surface-immobilized probe molecules is a process of fundamental importance across the clinical, biological, chemical, and nanosciences. For example, the molecular specificity between cDNA strands allows for the identification of unknown nucleic acid targets for genotyping and gene expression.[1,2] Similarly, the high specificity of antibodies[3–5] and aptamers[6,7] for discriminating between proteins and protein conformations can be used to understand, diagnose, and treat chronic illnesses better. Molecular specificity is also being explored increasingly as a route for directing the assembly of nanoscale objects, for example, carbon nanotubes,[8] quantum dots,[9] and nanowires,[10] into complex, integrated devices that are interfaced to the outside world.

In nature, the directed assembly of many macromolecular complexes is achieved via a number of distinct peptide motifs that regulate non-covalent protein–protein interactions. A notable example, the α-helical coiled coil, is an oligomerization motif thought to be present in 3–5% of all proteins[11] and involved in the assembly of a wide range of protein complexes, including many eukaryotic transcription factors. α-Helical coiled coils are formed by the association of two or more α-helical peptides into a stable, supercoiled complex.[12] Hydrophobic interactions between α-helical peptides (arising from hydrophobic residues at positions a and d of the helix heptad repeat sequence shown in Figure 1) produce most of the binding energy and provide stability to the coiled-coil complex. Stability is also regulated by electrostatic interactions between charged residues adjacent to the hydrophobic core at positions e and g. Critically, these electrostatic interactions also confer specificity and selectivity to the coil–coil interaction. For example, preferential pairing of the Fos and Jun leucine zipper is a result of repulsive, interhelical electrostatic interactions that effectively destablize the Fos homodimer in favor of heterodimer assembly.[13,14] This idea was explored further by O'Shea et al., who designed a synthetic coiled-coil complex that showed a greater than 10^5-fold preference for heterodimer over homodimer assembly.[15] Today, there exists a family of synthetic coiled-coil peptides that exhibit well-defined, heterospecific interactions with one another and that can be used as versatile, modular components for molecular engineering.[16–18]

Europe PMC Funders Author Manuscripts

Despite the prevalence of this biologically important motif, the generation of functional, peptide-derivatized surfaces and their use in organizing and directing the self-assembly of supramolecular structures has been largely neglected. Indeed, apart from a few notable examples,[19–21] the self-assembly of peptide-based materials on a surface has received very little attention, with investigations focusing instead on peptide folding in the solution phase. Here, for the first time, we use electrochemical impedance spectroscopy to evaluate the assembly, specificity, and affinity of coiled-coil heterodimers on the surface, where one of the peptides is first immobilized directly onto a gold electrode.

EXPERIMENTAL SECTION

Materials

All peptides were synthesized by PPR, Ltd. (Fareham, U.K.) at a purity >50% as determined by reversed-phase high-performance liquid chromatography (RP-HPLC) and stored lyophilized in a desiccator. Stock solutions of each peptide were made to a concentration of 1 mg/mL in 100 mM phosphate buffer at pH 7 and stored at 4 °C. Sequences of the peptides used in this study are BASE-C, AQLKKKLQANKKKLAQLKWKLQALKKKLAQGGGSC; ACID, AQLEKELQALEKELAQLEWENQALEKELAQ; BLK-C, SLDTLAEQLDPSANNVLSC; and Jun-C, IARLEEKVKTLKAQNSELASTANMLREQVAQLKQKVVMNHGGGSC.

Ethanol (99%) and isopropanol (99%) from Fisher (Loughborough, U.K.), acetone (98%), monosodium phosphate, monohydrate, disodium phosphate, heptahydrate, (3-mercaptopropyl)-trimethoxysilane, copper(II) perchlorate, sulfuric acid, and hydrogen peroxide from Sigma (Gillingham, U.K.), and *n*-doped silicon (100) capped with a 300 nm thick thermal oxide from Compart Technology (Peterborough, U.K.) were used as received.

Electrochemical Impedance Spectroscopy

Peptide layers were immobilized on a polycrystalline Au surface, and the electrochemical impedance was recorded with a Bio Logic VSP potentiostat using a conventional three-electrode cell with a Pt counter electrode and Ag/AgCl (saturated KCl) reference electrode. Impedance was measured at 0 V versus Ag/AgCl with a sinusoidal potential modulation of ±5 mV. The amplitude and phase shift of the resulting current were recorded over a frequency range spanning 6 decades (from 0.1 Hz to 100 kHz).

A combination of mechanical and electrochemical polishing was used to prepare the polycrystalline gold rod electrode surfaces for peptide functionalization. The rod electrodes (3 mm in diameter; BASi, Kenilworth, U.K.) were first polished mechanically using a range of alumina slurries of decreasing particle size (from 1.0 to 0.05 μm). The electrodes were then sonicated in acetone and ultrapure water (18.2 MΩ cm; Milli-Q systems) for 10 min each to remove residual alumina particles. Electrochemical polishing was performed in 0.1 M H_2SO_4 aqueous solution from −0.2 to +1.5 V versus Ag/AgCl at a scan rate of 0.1 V s^{-1}. The voltage scan was repeated until the cyclic voltammograms became stable and reproducible (typically 25 cycles). Finally, the electrodes were immersed in ultrapure water and absolute ethanol and sonicated for 10 min in each prior to incubation in peptide solution.

Europe PMC Funders Author Manuscripts

Ellipsometry

Peptide layers were immobilized on Au-coated glass slides, and the layer thickness was recorded using a Beaglehole Instruments picometer phase-modulated spectroscopic ellipsometer (Wellington, New Zealand). Measurements were taken at an angle of 70° and over a wavelength range of 300–800 nm with a measurement step size of 1 nm. Gold surfaces were fabricated by electron-beam evaporation to deposit a 20 nm thick titanium adhesion layer followed by a 150 nm thick gold layer under vacuum at a base pressure of 10^{-7} mbar onto standard microscope slides. Substrates were cleaned prior to metal deposition by immersion in Piranha solution (70% H_2SO_4 and 30% H_2O_2) for 10 min before sonicating in ultrapure water, ethanol, and isopropyl alcohol (IPA) for 10 min each. The freshly prepared substrates were placed into the peptide solution immediately following removal from the deposition chamber. The peptide functionalized substrates were dried under nitrogen gas prior to measurement. Measurements were performed on three different areas of the functionalized surface and repeated 3 times.

Circular Dichroism (CD)

CD measurements were carried out using a Chirascan CD spectrophotometer (AppliedPhotophysics, Leatherhead, Surrey, U.K.). Measurements were performed over a wavelength range of 180–280 nm with a measurement step size of 1 nm. The spectra of each sample was measured 20 times successively and averaged. All measurements were performed in 0.1 M phosphate buffer at pH 7 using a standard quartz cuvette (Hellma, Southend on Sea, U.K.).

RESULTS AND DISCUSSION

Peptide Immobilization

We investigated the on-surface assembly of the antiparallel ACID:BASE coiled-coil heterodimer developed by Oakley et al.[22] and based on the heterodimer design of O'Shea et al.[15] This synthetic coiled coil is based on the naturally occurring GCN4 leucine zipper but modified to include charged amino acids at positions e and g (glutamic acid in ACID and lysine in BASE) introduced to destabilize homodimer assembly at neutral pH. We further modified the BASE peptide to introduce a cysteine residue at the C terminus. This is the only cysteine in the peptide and allows for oriented, specific, and covalent attachment to a thiol-reactive surface. A flexible linker sequence (GGGS) commonly used in phage display[23] was also included between the unmodified BASE peptide and the cysteine. This provides the immobilized peptide greater flexibility and distances the coil–coil interaction region away from the surface. The modified BASE peptide, containing both the cysteine and flexible linker, is referred to as BASE-C. The results of a CD solution phase study into the formation of the BASE-C:ACID heterodimer at pH 7 are shown in Figure 1b. A pronounced helical structure was observed upon mixing of the BASE-C and ACID peptides as inidicated by CD minima at 222 and 208 nm. This is typical of the formation of a stable coiled-coil heterodimer. In contrast, CD spectra of the isolated ACID and BASE-C peptides show little evidence for helical content. These results compare well to previous CD experiments of coiled-coil heterodimers[15] and confirm that the cysteine and linker modifications have little or no negative impact on the assembly of the BASE-C:ACID heterodimer.

Having demonstrated stable heterodimer assembly in solution, we next used electrochemical impedance spectroscopy to investigate immobilization of the cysteine-modified peptide BASE-C onto the surface of an Au electrode. Typical impedance spectra of the cleaned Au surface before and after functionalization with BASE-C are shown in Figure 2. The electrode was functionalized by immersion in a 1 mg/mL solution of BASE-C for 18 h followed by rinsing in 100 mM phosphate buffer at pH 7. The impedance spectra were acquired *ex situ* in 10 mM phosphate buffer at pH 7. Critically, we see the magnitude of the electrochemical impedance, $|Z|$, increase by almost 2 orders of magnitude at 100 mHz following functionalization. This is consistent with the deposition of an ionic insulating layer on the Au surface. We also observe the phase angle, $\phi(z)$, of the derivatized electrode approach −90°, corresponding to an increase in capacitance, again supporting functionalization of the surface with an insulating layer. Despite impedance spectra characteristic of a functionalized surface, no significant changes in $|Z|$ or $\phi(z)$ were observed after exposing the derivatized electrode to a solution of the ACID peptide, as shown in Figure 2. Indeed, no measurable shifts in electrochemical impedance were observed even after extending the incubation time to 18 h or after increasing the concentration of the ACID peptide solution to 1 mM.

The apparent suppression of BASE-C:ACID heterodimer on-surface assembly may be understood by a more detailed analysis of the electrochemical impedance spectra. Bode plots of the BASE-C functionalized surface (Figure 2a) indicate typical values of $|Z| = 4 \times 10^4\ \Omega\ cm^2$ at 100 mHz. Although smaller than that observed for a pristine and defect-free self-assembled monolayer ($|Z|$ up to $10^5\ \Omega\ cm^2$ observed for an alkanethiol monolayer formed on Au),[24] the significant increase in $|Z|$ is commensurate with the formation of a molecular layer in which the peptides are immobilized at high grafting densities. This is further confirmed by the gradient of the Bode plot, which is calculated to be −0.9 for frequencies <50 Hz, close to the theoretical value of −1 expected for an electrode coated with a purely capacitive layer. Similarly, the minimum phase angle was found to be −84°, close to the theoretical limit of −90° for a Helmholtz ideal capacitor.[25,26]

Using a basic Randles circuit to simulate the impedance characteristics of Figure 2, we estimate the capacitance of the BASE-C peptide monolayer to be 1.3 $\mu F\ cm^{-2}$. This is comparable to the capacitance of an alkanthiol monolayer assembled on a polycrystalline Au surface.[24] Assuming that the dielectric constant for the peptide layer is around 3,[27,28] comparable to a monolayer of alkanethiols on gold, we thus calculate a BASE-C monolayer thickness of approximately 20 Å. We also used ellipsometry to measure more accurately the thickness of BASE-C assembled on an Au-coated glass slide. We found an average monolayer thickness of 29 Å. We note that the length of a 31 amino acid peptide folded into a α-helical conformation is expected to be 43 Å.[29,30] This measurement coupled with the frequency dependencies of $|Z|$ and $\phi(z)$ suggests the formation of a peptide monolayer that has self-assembled with high packing density onto the Au surface.

On-Surface Assembly of the Coiled-Coil Heterodimer

The efficiency of hybridization between a DNA target in solution and a complementary probe immobilized on a surface is strongly dependent upon the density of the immobilized DNA layer.[31,32] In particular, hybridization has been shown to be strongly suppressed by

electrostatic interactions and steric crowding that occur at high grafting densities.[33] Similarly, given the capacity of BASE-C to self-assemble into a densely packed peptide monolayer, we expect the efficiency of coiled-coil heterodimer assembly to be influenced by the density of the immobilized peptide.[34–36] We thus developed an approach for regulating the density of the immobilized BASE-C peptide by diluting the peptide monolayer with the 19 amino acid blocking peptide BLK-C.

Figure 3a shows the on-surface assembly of the BASE-C:ACID heterodimer monitored using electrochemical impedance spectroscopy. Here, the BASE-C layer was assembled onto the freshly prepared electrode surface from a 50%:50% solution of BASE-C:BLK-C. In contrast to the uniform 100% BASE-C functionalized surface, we now observe stable shifts in the electrochemical impedance following the addition of ACID and, in particular, a shift in the electrochemical phase, $\phi(z)$. Furthermore, we see that the magnitude of the shift in $\phi(z)$ is dependent upon the concentration of ACID and causes $\phi(z)$ to move toward −90° at frequencies <100 Hz, suggesting an increasingly capacitive layer.

This change in electrochemical impedance is more obvious when plotting the difference in phase, $\Delta\phi(z)$, before and after exposure to ACID. This is shown in Figure 3b for electrode surfaces functionalized from a 50%:50% solution of BASE-C:BLK-C solution following incubation with a 280 μM solution of ACID. Figure 3b also shows repeats of this experiment performed on three independent and identically functionalized electrodes. From these repeat measurements, we calculate a standard deviation, measured at 100 mHz of 0.18°. This is shown in the error bars of Figure 3c (black curve). Furthermore, Figure 3c clearly demonstrates that the change in $\phi(z)$ can be ascribed specifically and unambiguously to the formation of the BASE-C:ACID heterodimer. We observe stable shifts in the electrochemical phase angle only when a surface functionalized using a solution containing 50%:50% BASE-C:BLK-C is incubated with the specific coiled-coil partner, ACID. $\Delta\phi(z)$ remains close to zero for all other control experiments involving non-specific peptide interactions. The observed $\Delta\phi(z)$ is thus a measure of specific heterodimer assembly rather than a non-specific peptide interaction or nonspecific adsorption on the surface. We note that $\phi(z)$ remains constant [$\Delta\phi(z) \simeq 0$] following incubation of a surface functionalized with a second cysteine-modified peptide, Jun-C, with ACID, where Jun is known to form a stable heterodimer with the coiled-coil partner Fos. This suggests that no formation of the Jun-C:ACID heterodimer occurs and is consistent with CD measurements on solutions of Jun-C and ACID, shown in Figure 1c. Our electrochemical results of Figure 3 demonstrate conclusively that the specificity and selectivity associated with coiled-coil heterodimers is preserved even when assembly occurs on surface.

The data presented in Figure 3 is for a surface derivatized by incubation in a 50%:50% mixture of BASE-C:BLK-C. We also investigated heterodimer on-surface assembly for surfaces functionalized with different concentrations of BASE-C, as shown in Figure 4. At low concentrations (≤20% BASE-C in solution), any change in the electrochemical impedance of the layer is below the sensitivity of the measurement system, and we thus observe no shift in $\phi(z)$. Similarly, $\phi(z)$ remains constant at concentrations ≥70%, where electrostatic interactions and steric crowding in the self-assembled peptide monolayer inhibit dimer assembly. For our measurement system, we observe maximum sensitivity to BASE-

C:ACID heterodimer assembly for surfaces functionalized with BASE-C around 50% in solution.

CONCLUSION

We have demonstrated, for the first time, the use of electrochemical impedance spectroscopy to monitor the on-surface assembly of a *de novo* coiled-coil heterodimer. Immobilization is achieved via the introduction of a single cysteine residue at the C terminus of one peptide. While this ensures covalent, oriented, and stable attachment to the surface of an Au electrode, the high efficiency of the energetically favorable Au–S bond results in the immobilization of peptides at high grafting densities. Crucially, we show that the efficiency of dimerization between an α-helical peptide in solution and its complementary peptide immobilized on a surface is strongly dependent upon the density of the immobilized peptide layer. In particular, heterodimer assembly was found to be strongly suppressed with high-density peptide monolayers, likely because of steric crowding within the immobilized molecular layer. We thus demonstrate an approach for regulating the density of the immobilized BASE-C peptide by diluting the monolayer with a thiolated, random-coil peptide and demonstrate electrochemical detection of coiled-coil heterodimer on-surface assembly and with high specificity and, thus, pave the way for the use of synthetic peptides as versatile, modular components for molecular and bioelectronic engineering.

ACKNOWLEDGMENTS

Part of this research was supported by the Research Council UK's Basic Technology Programme. We are grateful for the support of the University of Leeds' Biomedical and Health Research Centre and the Institute for Bionanosciences, the UK EPSRC, the Royal Society, and the Wolfson Foundation. This work was partially funded through WELMEC, a Centre of Excellence in Medical Engineering funded by the Wellcome Trust and EPSRC, under Grant Number WT 088908/Z/09/Z.

REFERENCES

(1). Schena M, Shalon D, Davis RW, Brown PO. Quantitative monitoring of gene expression patterns with a complementary DNA microarray. Science. 1995; 270:467–470. [PubMed: 7569999]

(2). Lashkari DA, DeRisi JL, McCusker JH, Namath AF, Gentile C, Hwang SY, Brown PO, Davis RW. Yeast microarrays for genome wide parallel genetic and gene expression analysis. Proc. Natl. Acad. Sci. U.S.A. 1997; 94:13057–13062. [PubMed: 9371799]

(3). MacBeath G, Schreiber SL. Printing proteins as microarrays for high-throughput function determination. Science. 2000; 289:1760–1763. [PubMed: 10976071]

(4). Jones RB, Gordus A, Krall JA, MacBeath G. A quantitative protein interaction network for the ErbB receptors using protein microarrays. Nature. 2006; 439:168–174. [PubMed: 16273093]

(5). Parikh K, Peppelenbosch MP. Kinome profiling of clinical cancer specimens. Cancer Res. 2010; 70:2575–2578. [PubMed: 20332226]

(6). Evans D, Johnson S, Laurenson S, Davies AG, Ko Ferrigno P, Wälti C. Electrical protein detection in cell lysates using high-density peptide–aptamer microarrays. J. Biol. 2008; 7(1):3. [PubMed: 18237447]

(7). Bunka DHJ, Stockley PG. Aptamers come of age—At last. Nat. Microbiol. Rev. 2006; 4:588–596.

(8). Sanchez-Pomales G, Morales-Negron Y, Cabrera CR. Study of self-assembled monolayers of DNA and DNA–carbon nanotube hybrids. Rev. Adv. Mater. Sci. 2005; 10:261265.

(9). Weiss DN, Brokmann X, Calvet LE, Kastner MA, Bawendi MG. Multi-island single-electron devices from self-assembled colloidal nanocrystal chains. Appl. Phys. Lett. 2006; 88:143507.

Europe PMC Funders Author Manuscripts

(10). Nam KT, Kim DW, Yoo PJ, Chiang CY, Meethong N, Hammond PT, Chiang YM, Belcher AM. Virus enabled synthesis and assembly of nanowires for lithium ion battery electrodes. Science. 2006; 312:885–888. [PubMed: 16601154]

(11). Wolf E, Kim PS, Berger B. MultiCoil: A program for predicting two- and three-stranded coiled coils. Protein Sci. 1997; 6:1179–1189. [PubMed: 9194178]

(12). Liu J, Zheng Q, Deng Y, Cheng CS, Kallenbach NR, Lu M. A seven-helix coiled coil. Proc. Natl. Acad. Sci. U.S.A. 2006; 103:15457–15462. [PubMed: 17030805]

(13). O'Shea EK, Rutkowski R, Stafford WF, Kim PS. Preferential heterodimer formation by isolated leucine zippers from Fos and Jun. Science. 1989; 245:646–648. [PubMed: 2503872]

(14). O'Shea EK, Rutkowski R, Kim PS. Mechanism of specificity in the Fos/Jun oncoprotein heterodimer. Cell. 1992; 68:699–708. [PubMed: 1739975]

(15). O'Shea EK, Lumb KJ, Kim PS. Peptide velcro: Design of a heterodimeric coiled coil. Curr. Biol. 1993; 3:658–667. [PubMed: 15335856]

(16). Grant R, Keating A. Synthetic coiled-coil interactome provides heterospecific modules for molecular engineering. J. Am. Chem. Soc. 2010; 132:6025–6031. [PubMed: 20387835]

(17). Acharya A, Rishi V, Vinson C. Stability of 100 homo and heterotypic coiled-coil a–a′ pairs for ten amino acids (A, L, I, V, N, K, S, T, E, and R). Biochemistry. 2006; 45:11324–11332. [PubMed: 16981692]

(18). Ashkenasy G, Ghadiri MR. Boolean logic functions of a synthetic peptide network. J. Am. Chem. Soc. 2004; 126:11140–11141. [PubMed: 15355081]

(19). De Crescenzo G, Litowski JR, Hodges RS, O'Connor-McCourt MD. Real-time monitoring of the interactions of two-stranded de novo designed coiled-coils: Effect of chain length on the kinetic and thermodynamic constants of binding. Biochemistry. 2003; 42:1754–1763. [PubMed: 12578390]

(20). Stevens MM, Allen S, Sakata JK, Davies MC, Roberts CJ, Tendler SJN, Tirrell DA, Williams PM. pH-dependent behavior of surface-immobilized artificial leucine zipper proteins. Langmuir. 2004; 20:7747–7752. [PubMed: 15323527]

(21). Enander K, Aili D, Baltzer L, Lundstrom I, Liedberg B. α-Helix-inducing dimerization of synthetic polypeptide scaffolds on gold. Langmuir. 2005; 21:2480–2487. [PubMed: 15752043]

(22). Oakley MH, Kim PS. A buried polar interaction can direct the relative orientation of helices in a coiled coil. Biochemistry. 1998; 37:12603–12610. [PubMed: 9730833]

(23). Barbas, CF.; Burton, DR.; Scott, JK.; Silverman, GJ., editors. Phage Display: A Laboratory Manual. Cold Spring Harbor Laboratory Press; Cold Spring Harbor, NY: 2001.

(24). Boubour E, Lennox RB. Insulating properties of self-assembled monolayers monitored by impedance spectroscopy. Langmuir. 2000; 16:4222–4228.

(25). Helmholtz H. Studienüber electrische grenzschichten. Ann. Phys. 1879; 7:337–382.

(26). Boubour E, Lennox RB. Stability of ω-functionalized self assembled monolayers as a function of applied potential. Langmuir. 2000; 16:7464–7470.

(27). Rampi MA, Schueller OJA, Whitesides GM. Alkanethiol self-assembled monolayers as the dielectric of capacitors with nanoscale thickness. Appl. Phys. Lett. 1998; 72:1781–1783.

(28). Porter MD, Bright TB, Allara DL, Chidsey CED. Spontaneously organized molecular assemblies. 4. Structural characterization of n-alkyl thiol monolayers on gold by optical ellipsometry, infrared spectroscopy, and electrochemistry. J. Am. Chem. Soc. 1987; 109:3559–3568.

(29). Crick FHC. The packing of α-helices: Simple coiled-coils. Acta Crystallogr. 1953; 6:689–697.

(30). Ulijn RV, Woolfson DN. Peptide and protein based materials in 2010: From design and structure to function and application. Chem. Soc. Rev. 2010; 39:3349–3350. [PubMed: 20672166]

(31). Gong P, Levicky R. DNA surface hybridization regimes. Proc. Natl. Acad. Sci. U.S.A. 2008; 105:5301–5306. [PubMed: 18381819]

(32). Peterson AW, Heaton RJ, Georgiadis RM. The effect of surface probe density on DNA hybridization. Nucleic Acids Res. 2001; 29:5163–5168. [PubMed: 11812850]

(33). Castelino K, Kannan B, Majumdar A. Characterization of grafting density and binding efficiency of DNA and proteins on gold surfaces. Langmuir. 2005; 21:1956–1961. [PubMed: 15723495]

(34). Nuzzo RG, Allara DL. Adsorption of bifunctional organic disulfides on gold surfaces. J. Am. Chem. Soc. 1983; 105:4481–4483.

(35). Boncheva M, Vogel H. Formation of stable polypeptide monolayers at interfaces: Controlling molecular conformation and orientation. Biophys. J. 1997; 73:1056–1072. [PubMed: 9251822]

(36). Doneux T, Bouffier L, Mello LV, Rigden DJ, Kejnovska I, Fernig DG, Higgins SJ, Nichols RJ. Molecular dynamics and electrochemical investigations of a pH-responsive peptide monolayer. J. Phys. Chem. B. 2009; 113:6792–6799. [PubMed: 19366245]

Europe PMC Funders Author Manuscripts

Europe PMC Funders Author Manuscripts

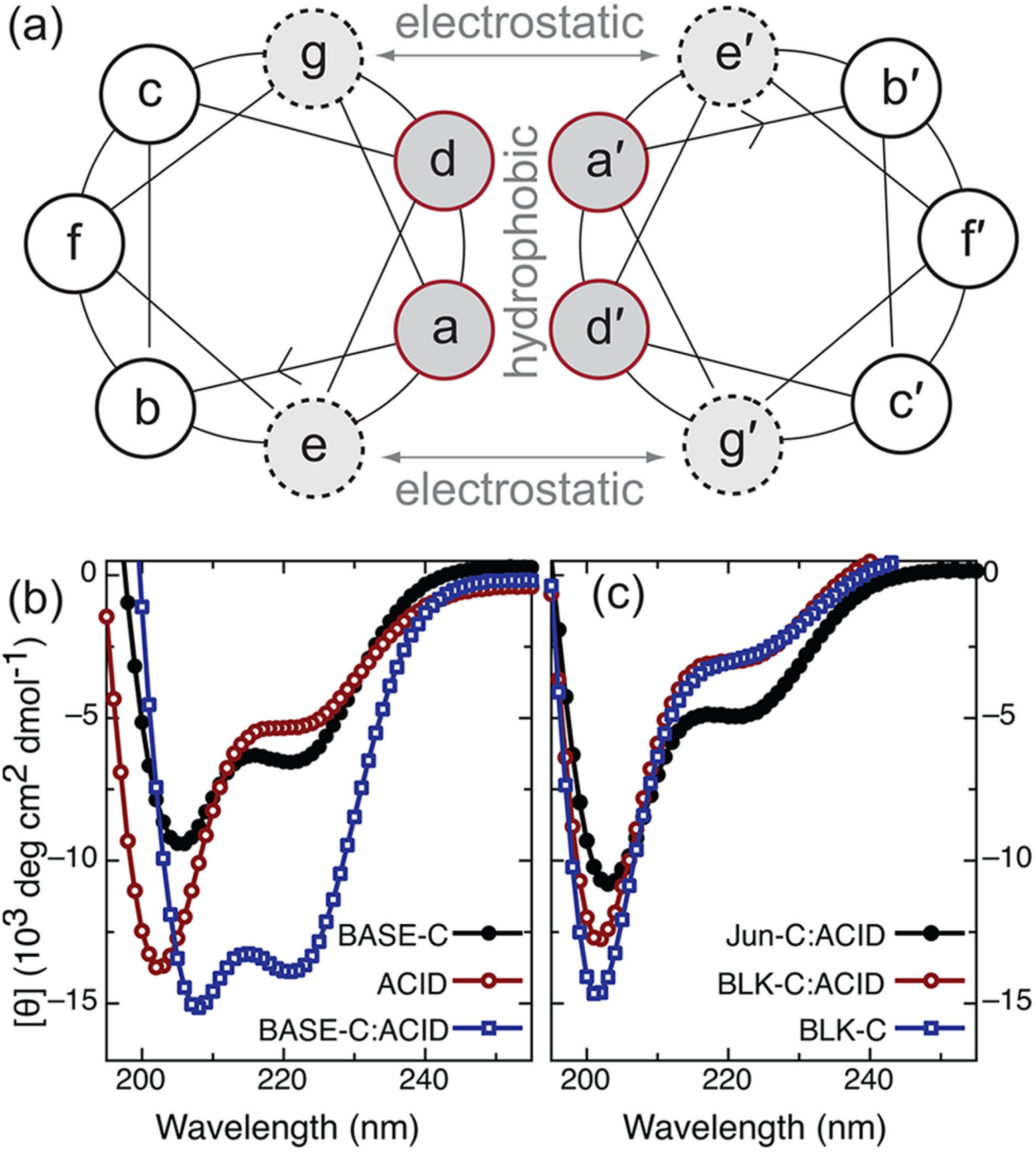

Figure 1.

(a) Helical wheel representation of the heptad repeat associated with a coiled-coil dimer. Dimer stability and specificity is regulated by a combination of hydrophobic interactions that occur between residues a and d and electrostatic interactions between amino acids at positions g and e. (b) Circular dichroism (CD) spectra for the individual peptides BASE-C and ACID and for the BASE-C:ACID heterodimer. (c) CD spectra for the random-coil peptide BLK-C and for solutions of BLK-C mixed with ACID and Jun-C mixed with ACID. For all CD measurements, peptides were dissolved in 0.1 M sodium phosphate at pH 7 at

0.25 mg/mL. For experiments involving mixed peptide solutions (i.e., BASE-C:ACID, BLK-C:ACID, and Jun-C:ACID), the solutions were allowed to incubate for 30 min at room temperature before the measurement was performed.

Europe PMC Funders Author Manuscripts

Europe PMC Funders Author Manuscripts

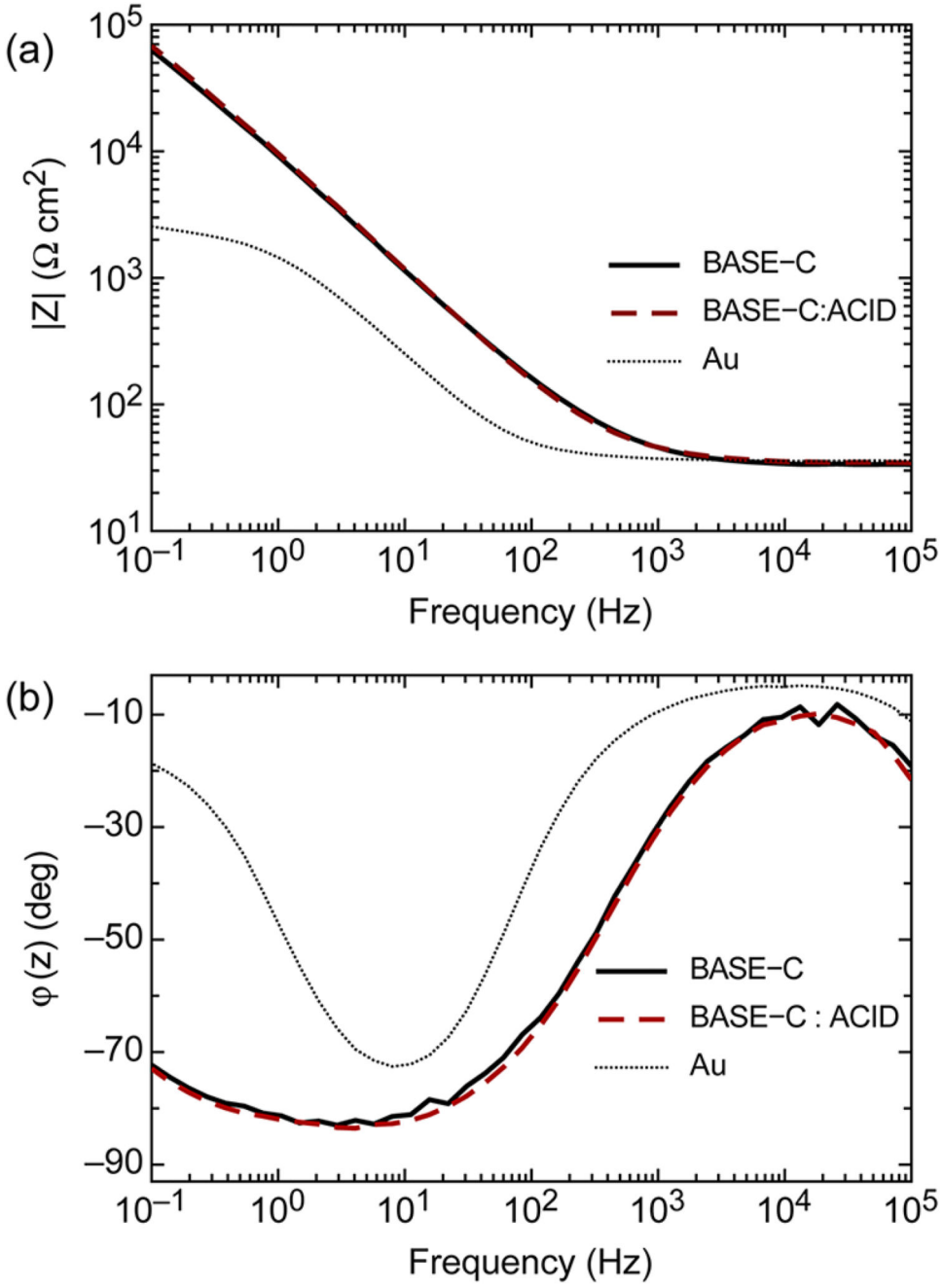

Figure 2.

Typical (a) Bode plot (log|Z| versus log *f*) and (b) Bode phase plot [$\phi(z)$ versus log *f*] of an Au electrode before and after functionalization with BASE-C and following incubation with a 200 μM solution of ACID for 60 min. All measurements were performed in 10 mM phosphate buffer at pH 7.

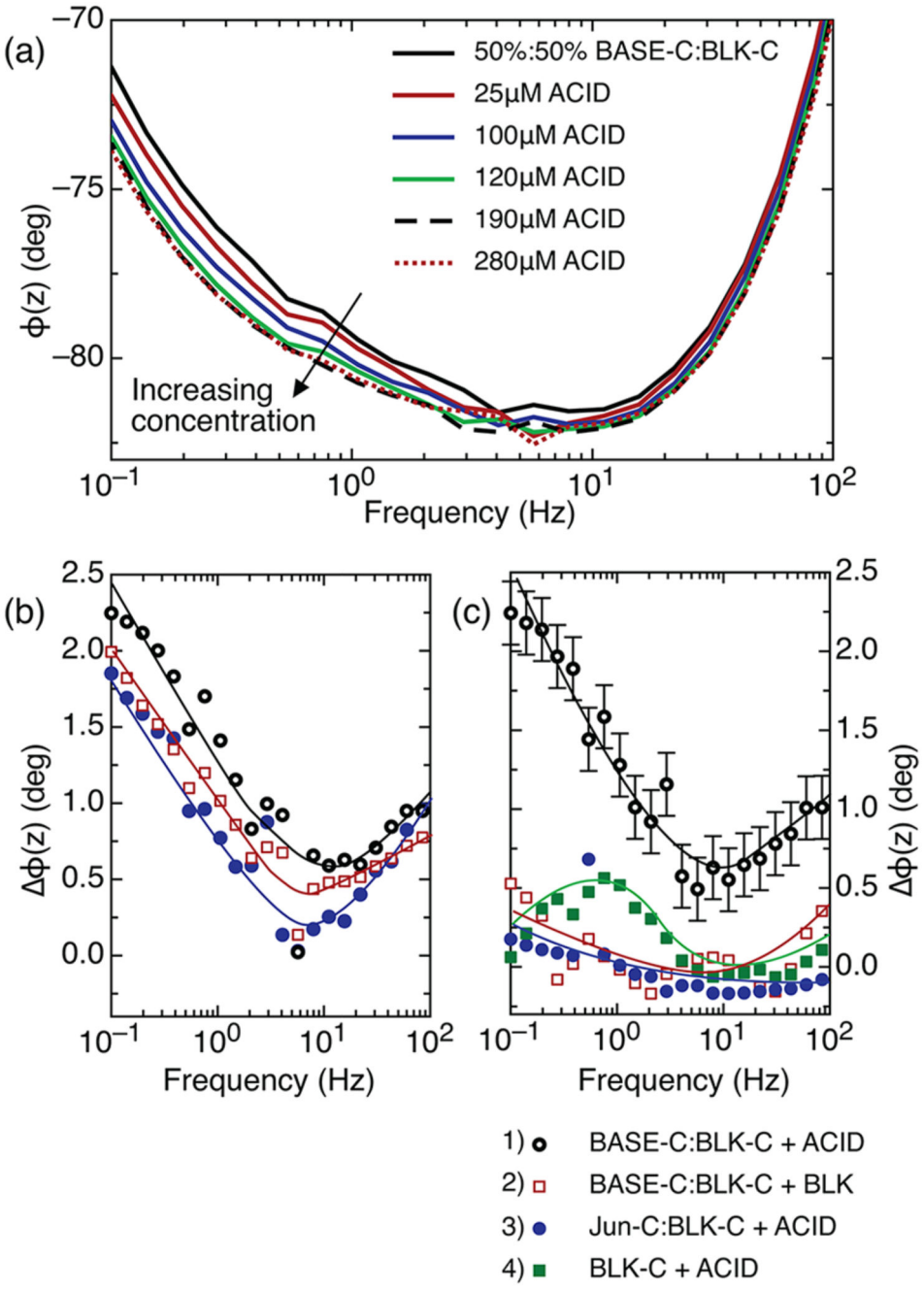

Figure 3.

(a) Frequency dependence of the phase of the electrochemical impedance for a surface functionalized using a solution containing 50%:50% BASE-C:BLK-C before and after incubation with increasing concentrations of ACID. (b) Frequency dependence of the difference in phase, $\Delta\phi(z)$, for a surface functionalized using a solution 50%:50% BASE-C:BLK-C as in panel a before and after incubation with 280 μM ACID. The three curves represent three independent measurements on three different surfaces. (c) $\Delta\phi(z)$ before and after incubation of functionalized surfaces with different peptides for (1) BASE-C:BLK-C +

ACID, incubation of a surface functionalized using a solution of 50%:50% BASE-C:BLK-C with 280 μM ACID; (2) BASE-C:BLK-C + BLK, incubation of a surface functionalized using a solution of 50%:50% BASE-C:BLK-C with 280 μM BLK; (3) Jun-C:BLK-C + ACID, incubation of a surface functionalized using a solution of 50%:50% Jun-C:BLK-C with 280 μM ACID; and (4) BLK-C + ACID, incubation of a surface functionalized with BLK-C with 280 μM ACID. Error bars show one standard deviation calculated from the multiple measurements shown in panel b.

Europe PMC Funders Author Manuscripts

Europe PMC Funders Author Manuscripts

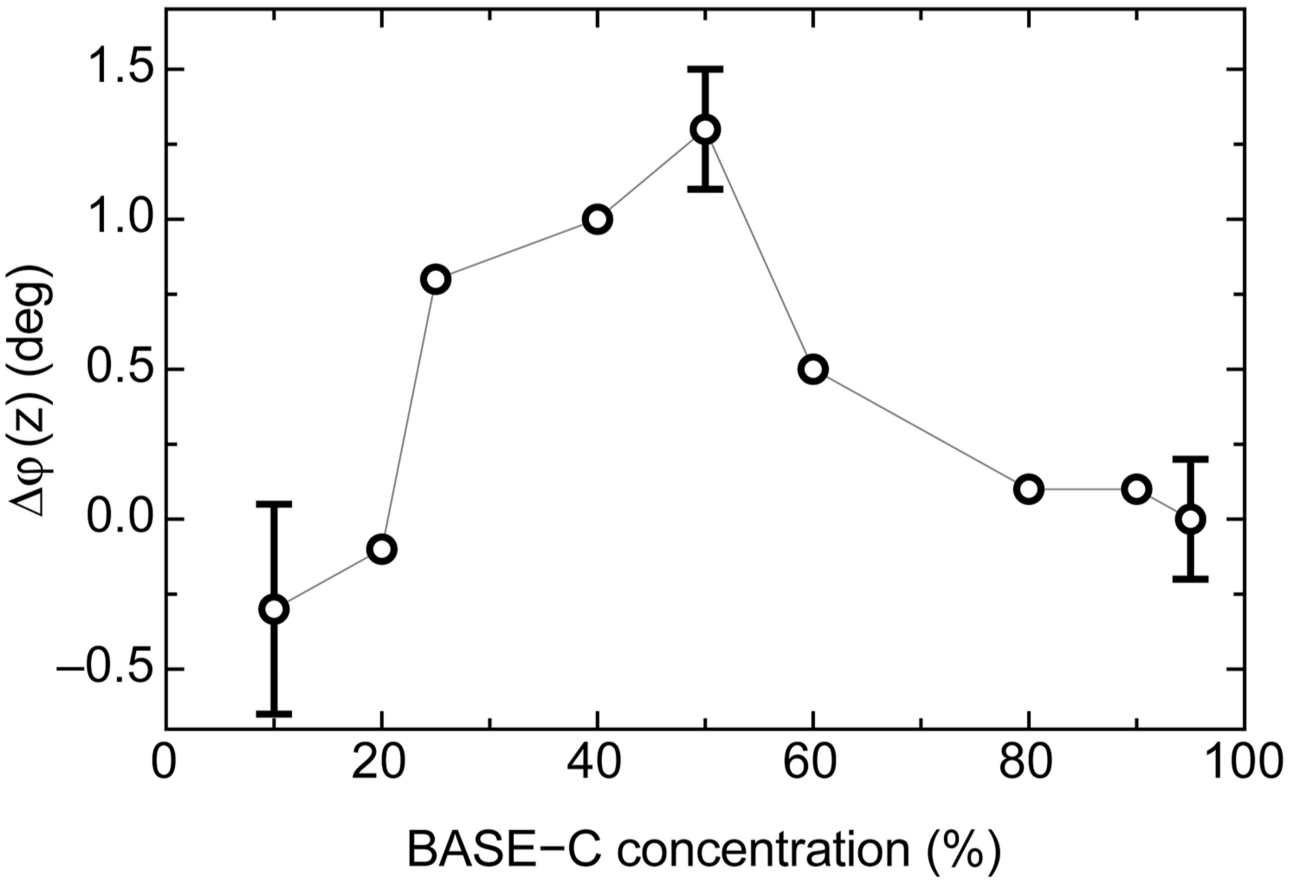

Figure 4.

Shift in the phase of electrochemical impedance, $\Delta\phi(z)$, as a function of the percentage of BASE-C peptide used in solution to functionalize the surface. Errors are calculated from three independent repeats of experiments performed using surfaces functionalized from solutions containing 0, 50, and 95% BASE-C.